ICA AIDED LINEAR SPECTRAL MIXTURE ANALYSIS OF AGRICULTURAL REMOTE SENSING IMAGES

*Naoko KOSAKA[*1] and Yukio KOSUGI[*2]*

[*1, 2.] Tokyo Institute of Technology, 4259, Nagatsudacho, Midori-ku, Yokohama-shi, 226-8502, Japan
E-mail: [*1] d02kosaka@pms.titech.ac.jp [*2] kosugi@pms.titech.ac.jp

ABSTRACT

In this paper, we propose a new method of estimating pure spectra and the mixture ratio by applying the Independent Component Analysis (ICA) to the agricultural remote sensing images for recognizing fine structure vegetation change on farmland, where the covering plant is unknown. This technique enables to separate the change of vegetation into qualitative one due to ecological characteristics such as the chlorophyll quantity, and the quantitative coverage one.

In the area of remote sensing several attempts using the ICA have been reported. These methods have defined the spectral reflectance pattern in the wavelength domain, as the independent component (IC), in order to extract pure spectra or only spectral features for the classification. In these cases, it is necessary to provide sufficient spectral bands to ensure the independence of each IC, as, for example, with hyperspectral images.

In our technique, we define the periodical spatial distribution of crops along the farmland position as the IC, so that pure spectra of crops are estimated as the mixture ratio of the IC, the coverage, unlike the conventional ones.

To the simulated mixed spectra, we demonstrated that this technique is useful even when the mixed spectra include vegetation covering fluctuation, additive noise such as thermal noise from the sensor and atmospheric noise, in the real data are involved.

In addition, by interpreting the coverage as the IC, it is possible to reduce the number of spectral bands. This means that our method can be applied not only to hyperspectral images but also multispectral images.

1. INTRODUCTION

Recently, several high-resolution imaging satellites are commercially available, and applications of remote sensing techniques in the field of agriculture, environment control, and disaster prevention are expected. However, in satellite and airborne sensor images obtained from high altitude, several materials exist in a single pixel, and the pixel value becomes the mixed one yielding the mixed spectrum. Therefore, various challenges have been made to estimate the pure material reflectance, i.e. the pure spectrum.

In the conventional remote sensing area, *a priori* knowledge of pure objects or pure spectra, which are included in the mixed spectrum and given by other measurement, are necessary to detect pure target objects and estimate mixture ratio from the observed mixed spectra[1][2][3][4]. Besides, several attempts using the ICA have been reported[5][6][7][8]. These have defined the spectral reflectance pattern, i.e. the pure spectrum against wavelength, as the IC to extract pure spectra or only spectral features for the classification. It is necessary to provide sufficient spectral bands to satisfy their independency, such as a hyperspectral image.

We define the periodical spatial distribution of crops, i.e. the coverage against the position, in a farmland as the IC, so that the pure spectra of crops are estimated as the mixture ratio of the IC, the coverage, differently from conventional ones. With this technique, it is possible to recognize both the qualitative change of crops from the estimated pure spectra, and quantitative one from the coverage.

This method also resolves the fluctuation of crop coverage and additive noise, such as thermal noise and atmospheric noise in the real data. These components cannot be removed just by raising the spatial resolution.

Moreover, using the coverage as the IC, it is possible to reduce the number of spectral bands. It means that our method could be applied not only to hyperspectral images but also multispectral images.

2. THE PERIODICAL MIXED SPECTRAL SEPARATION TECHNIQUE BY THE ICA

2.1. The formulation

In this section, we show the formulation of the ICA applied to a farmland model, according to the canonical form of ICA designed for separating the mixed signal observed from multiple sources at several positions into each original pure signal[9]. With the definition of the mixed signal $\mathbf{z} = (z_1, \ldots, z_k)^T$ and the mixing matrix A, consisting of k rows by l columns with element a_{ij}, the original signal $\mathbf{s} = (s_1, \ldots, s_l)^T$ satisfies,

$$\mathbf{z} = \mathbf{A} \cdot \mathbf{s} + \mathbf{n} + \mathbf{z_0}\ , \qquad \sum_{j=1}^{l} a_{ij} = 1, \tag{1}$$

where **n** is the additive noise. Though it is assumed that ICs have zero mean, in our farmland model, we define the constant term $\mathbf{z_0}$ as 'the direct current component', and identify it, which cannot be dissolved by the canonical form of the ICA. The ICA estimates **A** and **s** simultaneously under the conditions that (A) the mixed signal is a linear sum of original signals, (B) the probability density distribution of original signals are non-Gaussian, (C) the original signals are statistically independent. To calculate each a_{ij} in eq. (1), it should be $k \geq l-1$. By satisfying these simple conditions, the ICA enables us to estimate **A** and **s** simultaneously.

In this paper, we model the observation method in the farmland as Fig. 1, and generate simulated data. With wavelength λ and position x, the mixed spectra observed by the sensor are composed of two terms as,

$$I(\lambda,x)=I_0(\lambda)\cdot\{R_v(\lambda)\cdot\eta_v(x)+R_s(\lambda)\cdot\eta_s(x)\}\ , \qquad (2)$$

where $R_v(\lambda)$ and $\eta_v(x)$ are the pure spectra and the coverage of crops, and $R_s(\lambda)$ and $\eta_s(x)$ are those of soil, $I_0(\lambda)$ is the intensity of incident light. When only crops and soil exist in the single pixel, the following relation holds

$$\eta_v(x)+\eta_s(x)=1, \qquad (3)$$

where $\eta_v(x)$ and $\eta_s(x)$ consist of alternative current (AC) components which depend on position x, and direct current (DC) components which are independent of x as,

$$\eta_v(x)=\eta_v^{AC}(x)+\eta_v^{DC}\ ,\quad \eta_s(x)=\eta_s^{AC}(x)+\eta_s^{DC}\ , \qquad (4)$$

where $\eta_v^{AC}(x)$ and $\eta_s^{AC}(x)$ are AC components, and η_v^{DC} and η_s^{DC} are DC ones.

In our method, each parameter is interpreted as the ICA parameter shown in Table 1. By substituting eq. (3) into eq. (2), the problem reduces to eq. (5), i.e. one channel estimation for the dependency on $\eta_v(x)$.

$$I(\lambda,x)=I_0(\lambda)\cdot\left[\{R_v(\lambda)-R_s(\lambda)\}\cdot\eta_v(x)+R_s(\lambda)\right]\ . \qquad (5)$$

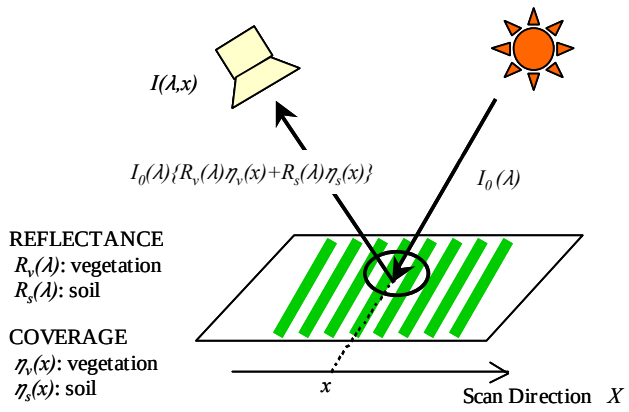

Fig. 1: An observation of a mixed spectrum.

Table 1: Parameters interpreted as ICA.

	in our method	in the ICA
λ	wavelength	position of observation
x	center position of the circular window	time
$R_v(\lambda), R_s(\lambda)$	reflectance	mixture ratio
$\eta_v(x), \eta_s(x)$	coverage	independent component

In addition, we can suppose additive Gaussian noise to simulate real observations as,

$$I(\lambda,x)=I_0(\lambda)\cdot\left[\{R_v(\lambda)-R_s(\lambda)\}\cdot\eta_v(x)+R_s(\lambda)\right] + R_n(\lambda)\cdot\eta_n(x)\ . \qquad (6)$$

Where $R_n(\lambda)$ and $\eta_n(x)$ denote the amplitude and the periodical pattern of the noise respectively. Moreover, it is also necessary to consider fluctuations in coverage term, since the size of each crop might be irregular.

$$\eta_v(x)\ =\eta_v(x)+\Delta\eta_v(x). \qquad (7)$$

Considering the noise component and the coverage fluctuation, the observed mixed spectra are described by substituting eq. (4) and eq. (7) into eq. (6) as bellow,

$$\begin{aligned} I(\lambda,x) &= I_0(\lambda)\cdot\left[\{R_v(\lambda)-R_s(\lambda)\}\right. \\ &\quad \left.\{\eta_v^{AC}(x)+\eta_v^{DC}+\Delta\eta_v(x)\}+R_s(\lambda)\right] \\ &\quad + R_n(\lambda)\cdot\eta_n(x) \\ &= \mathbf{A}\cdot\mathbf{s}+\mathbf{n}+\mathbf{z_0}\ , \end{aligned} \qquad (8)$$

where

$$\begin{aligned} \mathbf{A}\cdot\mathbf{s} &= I_0(\lambda)\cdot\{R_v(\lambda)-R_s(\lambda)\}\{\eta_v^{AC}(x)+\Delta\eta_v(x)\}, \\ \mathbf{n} &= R_n(\lambda)\cdot\eta_n(x), \\ \mathbf{z_0} &= I_0(\lambda)\cdot\{R_v(\lambda)-R_s(\lambda)\}\cdot\eta_v^{DC}+I_0(\lambda)\cdot R_s(\lambda)\ . \end{aligned} \qquad (9)$$

When the ICA of eq. (1) is applied, the periodical signals, i.e. AC components depending on x, are estimated as the IC or noise, and the residual components without the periodicity as the DC component. As an effect of the ICA, the coverage term seems to be separable as long as its histogram remains within the Gaussian distribution.

2.2. Determination of the calibrating coefficient and the residual component

In this section, we show the process to extract mixture ratio and pure spectra by determining the calibrating coefficient and the DC component in eq. (8).

2.2.1. The derivation of invariant parameter

We propose a method for deciding the arbitrariness of the proportion of ICs and mixture ratio. We should identify this proportion to resolve the one channel ICA. It is necessary to account for the residual term of eq. (9) in order to separate the spectral term $\{R_v(\lambda)-R_s(\lambda)\}$ and coverage $\eta_v(x)$. That is to say, we specify the calibrating

coefficient to be used for separating **s** and **A** in eq. (8). As the technique for deciding the calibrating coefficient, we considered the following possibilities,

1. use of higher spatial resolution images for acquiring the covering pattern,
2. to calibrate at the wavelength where the spectral reflectance of the vegetation and the soil are stable,
3. to calibrate at the wavelength where the derivative of spectral reflectance of the vegetation and the soil are stable.

In this paper, we adopted the last method. Then the arbitrariness is removed by applying the same calibrating coefficient to other wavelengths.

When we employ hyperspectral data, vegetation and soil spectra are generally shown as in Fig. 2, in which x is the wavelength and y is the spectral reflectance. In the case of vegetation, the positions of peaks and valleys of the spectral reflectance decide the wavelength, at which the derivative becomes 0 with respect to λ. At the same wavelength, the derivative of the soil is considered as a constant value shown in Fig.3, since the spectral reflectance changes smoothly.

We may use the most stable single wavelength, however, the soil reflectance may fluctuate because of dispersion due to soil types and moisture content. Therefore, to obtain more stable calibration, which is universal for the soil of various types and conditions, we combine the derivative values at multiple wavelengths.

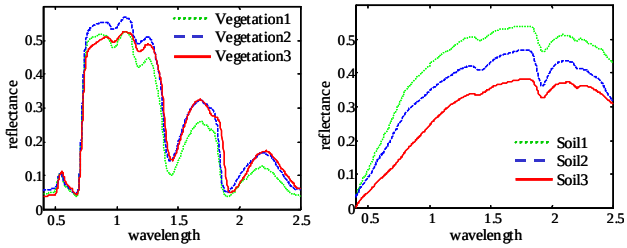

(1) Vegetation (2) Soil

Fig.2: Reflectance.

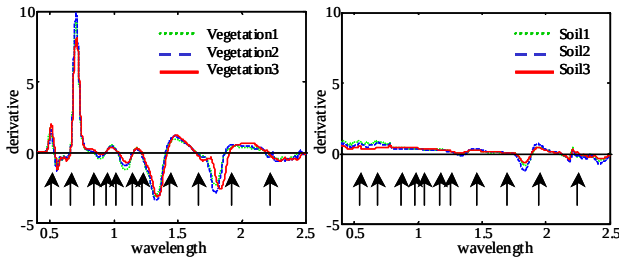

(1) Vegetation (2) Soil

Arrows indicate the wavelength at which the derivative of vegetation becomes zero.

Fig.3: Derivative of reflectance.

To decrease the dispersion in the multidimensional derivative feature space, we applied a multi dimensional inference technique.

First, we chose candidate wavelengths, where derivatives of soils are mostly constant and those of vegetation are close to zero. Next, we added the optimization process, which decreases the dispersion and increases the absolute value, since there is the dispersion of derivatives at those wavelengths. This process involves the discriminant analysis by using the mirror matrix in order to reduce the error effect of the vegetation zero derivatives.

Spectral reflectance and derivative of the soil at the wavelength in which the derivative of the vegetation becomes 0 are shown as bellow,

$$\begin{aligned}\mathbf{R}_j &= \left(R_j(\lambda_1), R_j(\lambda_2), R_j(\lambda_3), \ldots, R_j(\lambda_l)\right) \\ \mathbf{R}'_j &= \left(R'_j(\lambda_1), R'_j(\lambda_2), R'_j(\lambda_3), \ldots, R'_j(\lambda_l)\right).\end{aligned} \tag{10}$$

Here, the type of a soil is designated as $j = 1,2,...m$. Next, we define class1 to be consisted of the second equation of eq. (10). Then, the mirror matrix is defined to be class2.

$$\begin{aligned}\mathbf{Class1} &= \left\{\mathbf{R}'_1, \mathbf{R}'_2, \mathbf{R}'_3, \ldots, \mathbf{R}'_m\right\} \\ \mathbf{Class2} &= -\mathbf{Class1} = \left\{-\mathbf{R}'_1, -\mathbf{R}'_2, -\mathbf{R}'_3, \ldots, -\mathbf{R}'_m\right\}.\end{aligned} \tag{11}$$

To the above two classes, the discriminant analysis is applied. Taking the eigenvector of the medial axis transformation as B, new parameters will be obtained as,

$$\mathbf{R}'^{new}_{\mathbf{j}} = \mathbf{B} \cdot \mathbf{R}'_{\mathbf{j}} \,. \tag{12}$$

In Fig.4, the distributions before and after the discriminant analysis are shown. By this optimization process, we obtain the value, whose absolute value is large and the deviation is small, as the first component of discriminant analysis. It becomes possible that stabilized value, which is hardly affected by soil type and soil condition, is obtained. That is to say, the derivative is treated as if it was an intensity value in eq. (8).

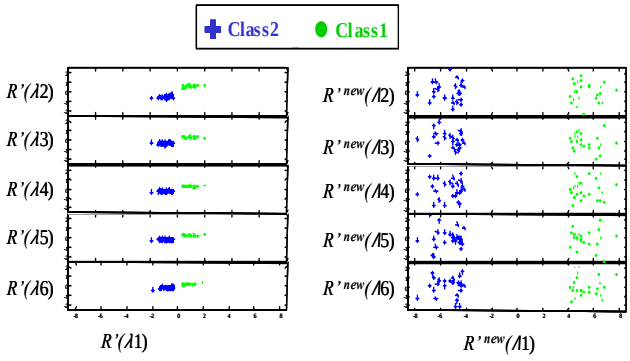

(1) Before the analysis (2) After the analysis

Fig.4: The discriminant analysis by the mirror matrix of the derivatives in case of soil.

2.2.2. The decision of the calibrating coefficient K

In this section, we show the procedure for obtaining the calibrating coefficient. In eq. (8), the ICA is applied to the AC component, to estimate the mixture ratio **A** and the IC **s** . Therefore, the calibrating coefficient is obtained using invariant parameter Ref_1^{new} of eq. (12) as follows,

$$I_0(\lambda)\cdot\{\,R_v(\lambda)-R_s(\lambda)\,\}\cdot\{\eta_v^{AC}(x)+\Delta\eta_v(x)\}=\mathbf{A}\cdot\mathbf{s}, \quad (13)$$

$$K\cdot\mathbf{A}=R_v'^{\,new}(\Lambda 1)-R_s'^{\,new}(\Lambda 1). \quad (14)$$

When we suppose $I_0(\lambda)=1$, the mixed spectra can be interpreted as spectral reflectance. The new mixture ratio and the IC become,

$$\begin{aligned}\mathbf{A}^{new}&=K\cdot\mathbf{A}\\ \mathbf{s}^{new}&=(1/K)\cdot\mathbf{s}\ .\end{aligned} \quad (15)$$

2.2.3. The decision of the direct current component

In this section, we consider the DC component. In eq. (8), we can eliminate the AC component by obtaining the mean value with respect to x. Eq. (15) is substituted into eq. (8), to yield the relationship with η_v^{DC} as,

$$\begin{aligned}&mean\{I(\lambda,x)\}\\ &=I_0(\lambda)\cdot\left[\{\,R_v(\lambda)-R_s(\lambda)\,\}\cdot\eta_v^{DC}+R_s(\lambda)\right]\\ &=\mathbf{A}^{new}\cdot\eta_v^{DC}+R_s(\lambda)\ .\end{aligned} \quad (16)$$

The invariant parameter is utilized here as well as the calibrating coefficient. And $mean\{I(\lambda,x)\}$ is obtained by averaging the mixed spectra of the input. The calibrating coefficient, mixture ratio, the ICs, and the DC component are substituted into eq. (8), then pure spectra, $R_s(\lambda)$ and $R_v(\lambda)$, are obtained.

2.3. The analysis procedure

The ICA is applied to eq. (8) as explained in section 2.2. In the procedure of Fig.5, pure spectra and the coverage are derived for vegetation and soil. Though mixed spectra of two objects were described in this paper, it is possible to increase the number of ICs as long as its histogram remains within the Gaussian distribution.

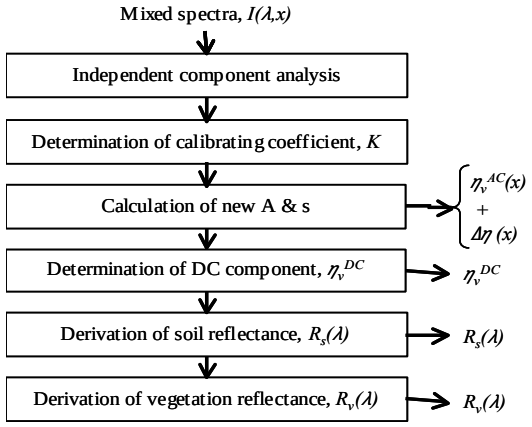

Fig.5: The derivation of coverage and pure spectra.

3. EXPERIMENTAL CONSIDERATION

First, we explain the method for generating simulated data of crop covering pattern used for the experiment. Then, the experimental result is shown. We used the package of Fast ICA in MATLAB opened to public[10].

3.1. The model of crop covering pattern

3.1.1. The periodical covering pattern

The length between ridges and crops in farmland is determined at a certain value in order to produce crops of the uniform size. Therefore, the covering pattern of crops and background soil is uniform in a same field. We approximate the receptive field of a sensor as the circular window shown in Fig.6. Depending on position x of the observation window, the coverage of crops changes periodically. The coverage of vegetation is described as bellow,

$$\eta_v=\{S_v+S(d1)+S(d2)\}/S(W_p), \quad (17)$$

here, $d1$ is the distance from the left end of the observation window to the right end of the crop area, and $d2$ is from the right end of the window to the left end of the crop area.

The coverage with respect to x for crop and soil are shown in Fig.7, indicating the periodicity and non-Gaussian distribution, which is the must in the ICA.

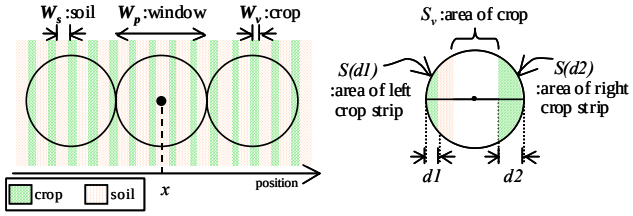

(1) Scanning (2) Calculation

Fig.6: The circular window model.

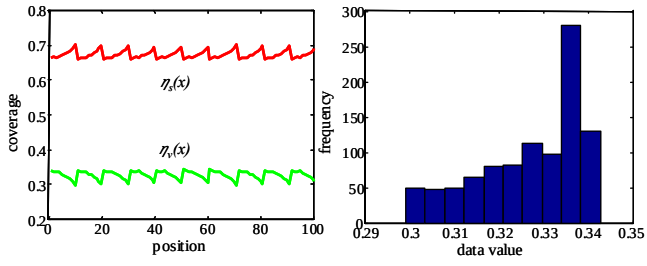

(1) Periodicity (2) non-Gaussian

Fig.7: Features of coverage η .

Where, parameters are supposed as, W_p : 250 cm, W_v : 21 cm, and W_s : 40cm.

3.1.2. The noise component

The thermal noise of the sensor is considered as additive Gaussian noise.

Although atmospheric noise consists of both multiplicative and additive components, in a limited narrow area of a certain crop field, atmospheric condition is almost uniform. Therefore, atmospheric noise for each band can be approximated as an additive Gaussian noise.

3.1.3. The fluctuation component of coverage

In the experiment, we use Gaussian distribution as a fluctuation component of the covering. We suppose a small fluctuation in the amplitude, which does not disturb non-Gaussian distribution of the original signal.

3.2. The input signal

The spectral profiles of vegetation are almost similar. Then, the spectrum of Conifer was adopted from the Johns Hopkins University (JHU) spectral library[11]. The soil spectrum is also chosen as the loam from the same library. Each pure spectrum is shown in Fig.8. We use these spectra as a standard in a field, where those objects have spectral dispersion in real data. There are 53 bands from visible to near infrared wavelength, with 20nm sampling between each band.

In order to stabilize derivatives, the 54th element is used as invariant derivative term for obtaining the calibrating coefficient. The derivative term of the soil adopted the value calculated from 25 types of soil in the JHU library, and the derivative term of crops was supposed to be 0.

3.3. Experimental results

3.3.1. Results without noise and fluctuation

Fig.9 shows the estimated pure spectra and the coverage. The detailed shape of each pure spectrum is estimated at the good accuracy with the average error of 1%, max 4%. Besides, the AC component on the coverage shows almost the same profile and the average error of the DC component is less than 1% and max 1%. It was

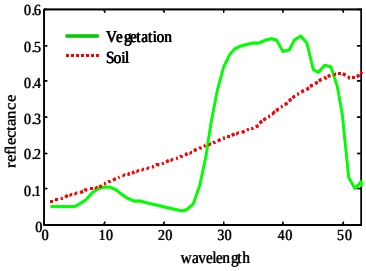

Fig.8: Pure spectra.

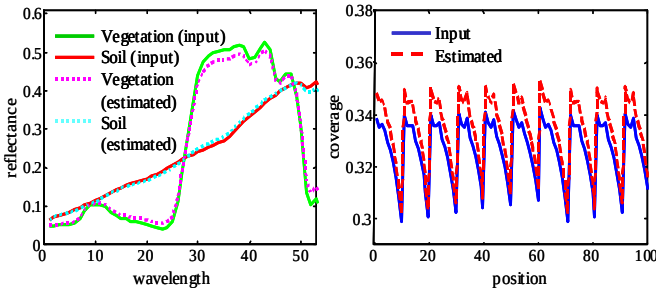

(1) Pure spectra (2) Coverage

Fig.9: Result without noise and fluctuation.

confirmed that the method enables us to distinguish objects, which have differences more than a few percents.

3.3.2. Results with noise and fluctuation

In Fig.10, the coverage, the noise, and the fluctuation components are shown. The noise amplitude is supposed as a few times larger than that of the periodical coverage change.

We confirmed that the probability distribution was separated into non-Gaussian part of the coverage and the Gaussian noise in Fig.11, when the ICs are estimated. Fig.12 shows the estimated pure spectra and the coverage. We confirmed that our method could estimate at the good accuracy with the average error of 2% and maximally 5%, even in the cases that noise and fluctuation components are involved. Besides, the AC component on the coverage shows almost the same profile and the average error of the DC component is less than 1% and 2% at the max.

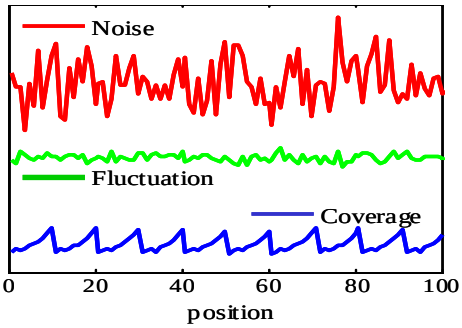

Fig.10: Amplitude.

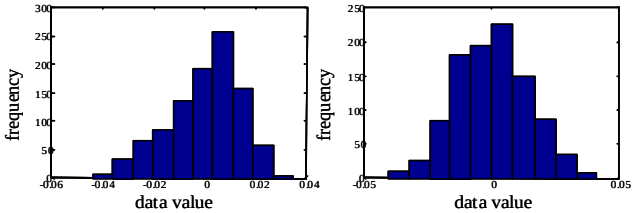

(1) Coverage (2) Noise

Fig.11: Histogram of independent components.

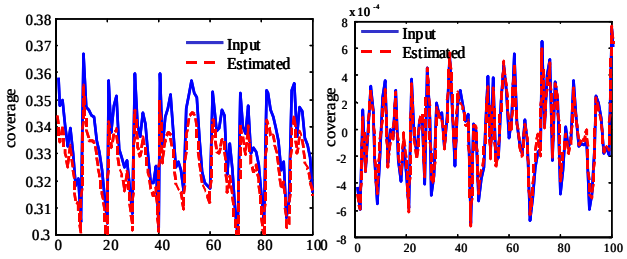

(1) Coverage (2) Noise

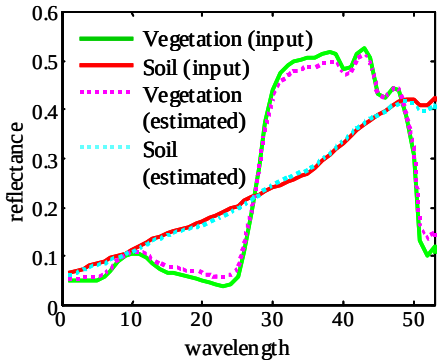

(3) Pure spectra

Fig.12: Result with noise and fluctuation.

4. DISCUSSION AND CONCLUSIONS

In the remote sensing field, several attempts using the ICA[5][6][7][8] have been reported. Differently from our method, these have defined the spectral reflectance pattern in the wavelength domain as the IC to extract pure spectra or only spectral features for the classification. In our technique newly proposed, the periodical spatial distribution of crops, the coverage, is defined as the IC, so that pure spectrum of crops is estimated as mixture ratio of the IC, the coverage.

We tested the new method of estimating pure spectra and mixture ratio by applying the ICA to the simulated mixed spectra. In the simulation, we supposed that the field under consideration is flat and the summation of a_{ij} in eq. (1) should be 1.0. We demonstrated that this technique is useful even under the condition that the mixed spectra include the vegetation covering fluctuation, and additive noise such as thermal sensor noise and atmospheric noise, which might be involved in real data.

In the future, more effective sampling method might be introduced while applying this technique to real remote sensing images. To ensure the adequate periodicity, we have to collect input data in different direction against the ridge in a farmland.

Moreover, this technique is applicable to the recognition of periodically distributed covering patterns observed through fiberscope, microscope, or semiconductor inspection machineries, etc.

ACKNOWLEDGMENT

The authors would like to thank Dr. Taichi Nakamura, Dr. Ushio Inoue and Dr. Sanae Miyazaki of NTT data Co., for giving us the opportunity and support to do this work.

REFERENCES

[1] R. L. Huguenin, M. A. Karaska, D. Van Blaricom, and J. R. Jensen,"Subpixel Classification of Bald Cypress and Tupelo Gum Tree in Thematic Mapper Imagery," Photogrammetric Engineering & Remote Sensing, Vol.63, pp.717-725, 1997.

[2] J. P. Kerekes and J. E. Baum, "Spectral Imaging System Analytical Model for Subpixel Object Detection," Vol.40, No.5, pp.1088-1101, 2002.

[3] C. I. Chang, "Target Signature-Constrained Mixed Pixel Classification for Hyperspectral Imagery," IEEE Trans. On Geoscience and remote sensing, Vol.40, No.5, pp.1065-1081, 2002.

[4] A. Moody, S. Gopal, and A. H. Strahler, "Artificial Neural Network Response to Mixed Pixels in Coarse-Resolution Satellite Data," Remote Sens. Environ., Vol.58, pp.329-343, 1996.

[5] X.Zhang and C.H.Chen, "New independent component analysis method using higher order statistics with application to remote sensing images," Opt.Eng, 41(7), pp.1717-1728, 2002.

[6] C.I.Chang, "Linear Spectral Random Mixture Analysis for Hyperspectral Imagery," IEEE Trans. On Geoscience and Remote Sensing, Vol.40, No.2, pp.375-392, 2002.

[7] T.M.Tu, "Unsupervised signature extraction and separation in Hyperspectral images: a noise-adjusted fast independent component analysis approach," Opt. Eng, 39(4), pp.897-906, 2000.

[8] L. Parra, K. R. Mueller, C. Spence, A. Ziehe, and P. Sajda, "Unmixing Hyperspectral Data," Advances in Neural Information Processing Systems 12, MIT Press, pp. 942-948, 2000.

[9] A. Hyvärinen, J. Karhunen and E. Oja: "Independent Component Analysis," John Wiley & Sons, 2001.

[10] E. Oja, "FastICA package for MATLAB," http://www.cis.hut.fi/~aapo/pub.html#FastICA/

[11] Johns Hopkins University Spectral Library, http://asterweb.jpl.nasa.gov/speclib/